AIAA Guidance, Navigation, and Control Conference and Exhibit
5-8 August 2002, Monterey, California

AIAA 2002-4450

DESIGNING ROBUST LARGE ENVELOPE FLIGHT CONTROLLERS FOR HIGH-PERFORMANCE AIRCRAFT

Paul Blue*, Dirk Odenthal# and Michael Muhler#

*Control Science and Dynamical Systems Center
University of Minnesota – Minneapolis

#Robust Control Group, Institute of Robotics and Mechatronics
German Aerospace Center (DLR) - Oberpfaffenhofen

Abstract

A simple two-degree-of-freedom control architecture and recent advanees in MIMO H_∞ parameter-space control design are combined to form a new method of designing large envelope flight controllers for high performance aircraft. The procedure enables the designer to explicitly define the desired closed-loop dynamics and guarantees that the closed-loop provides robust stability and robust performance, which are defined using MIMO H_∞ specifications. The result is a straightforward procedure that enables the design of a robust flight controller that "forces" the closed-loop dynamics to behave like the specified 'desired dynamies' despite disturbances, modeling uncertainties, and variations in aircraft dynamics due to changing flight conditions. The procedure is presented by designing an LTI pitch-rate controller for the F-16 Variable Stability In-Flight Simulator Test Aircraft (VISTA). Linear and nonlinear simulations show that the LTl controller provides predicted 'Level 1' flying qualities throughout the large design flight envelope.

1. Introduction

Designing flight control systems for high-performance military aircraft is an extremely demanding task. The controller must satisfy stringent performance specifications[12] throughout a large flight envelope despite large variations in the aircraft dynamics, which change significantly with flight condition. Due to these large variations in the dynamics, it is often impossible to design a fixed (i.e. LTI) controller that provides the required level of performance throughout the flight envelope. As a result, it is often necessary to use a gain-scheduled controller. Unfortunately, designing gain-scheduled controllers is a very complex chore. A "classical" method that has been successfully used to obtaining gain-scheduled controllers is to design LTI controllers at several trim points throughout the flight envelope, and then schedule them with operating condition; however, this is very tedious and becomes extremely complex when "modern" design methods are used to obtain the LTI controllers. The difficult task of traditional gain-scheduling has resulted in a significant amount of research over the past decade to develop methods of designing linear parameter-varying (LPV) controllers, which are "automatically" gain-scheduled (e.g. [11, 4, 16, 18, 10, 6]), and methods of "blending" (i.e. scheduling) multiple LPV controllers (e.g. [10,17]). While these LPV control design methods do provide a fairly systematic way of designing automatically gain-scheduled controllers, they are still quite involved and result in complex controllers, which are often conservative.

In [5], a much simpler approach for designing large envelope flight controllers was presented that provided the desired performance throughout the design envelope without gain-scheduling. The procedure combined a two-degree-of-freedom (2DOF) control architecture based on what is often referred to as a disturbance observer[15,19] and parameter-space control design techniques[2,14]. Parameter-space methods were used to design a large envelope pitch-rate controller for the F-16 VISTA by mapping SISO H_∞ stability and performance specifications into the "free" parameter-space of the 2DOF controller. Nonlinear simulations of VISTA with the resulting LTI controller predicted 'Level 1' flying qualities throughout the design envelope. However, since only SISO H_∞ specifications were considered, robust performance (with respect to the unstructured uncertainty) could not be guaranteed during the design. Of course, a robustness analysis of the resulting controller could be conducted after the design to determine whether or not it guaranteed robust performance, but it couldn't be guaranteed during the design.

In this paper, the large envelope flight control design method presented in [5] is extended to enable the treatment of MIMO H_∞ specifications, which enables robust performance to be guaranteed during the control design. The procedure combines the 2DOF control architecture used in [5] and recent advances in MIMO H_∞ parameter-space control design[1] to form a new approach for designing flight controllers for high performance aircraft. The combination of this control architecture and control design method form a simple, yet powerful design procedure. The controller

architecture is extremely attractive for a number of reasons, most notably, its insensitivity to disturbances and model uncertainty and its unambiguous structure, which enables the explicit definition of the desired closed-loop dynamics. The parameter-space control design method is attractive because of the transparency that it provides when mapping design specifications (H_∞ or other) into the free parameter-space of a fixed control architecture and its explicit, non-conservative treatment of real parameter variations (e.g. changing flight condition). The result is a straightforward method of designing large envelope flight controllers for high performance aircraft that satisfy MIMO H_∞ specifications (e.g. robust performance) throughout the design flight envelope without gain-scheduling. It is possible, of course, that for a given aircraft and a given set of design specifications that there is no LTI controller which can satisfy the specifications over the design envelope; however, we have found that the procedure presented here can often yield an LTI controller that guarantees robust performance over a large flight envelope even when other methods (e.g. "traditional" H_∞ and μ-synthesis via DK iteration) cannot. This is largely due to the parameter-space method's non-conservative treatment of the real parameters. The proposed design procedure is presented by designing a pitch-rate controller for the F-16 VISTA that provides predicted 'Level 1' handling qualities over a large design envelope with guaranteed H_∞ robust performance.

The remainder of the paper is organized in four main sections. An LPV model of the F-16 VISTA and the F-16 pitch-rate control design objectives are reviewed in Section 2. The proposed large envelope flight control design procedure is presented in Section 3 by designing a robust pitch-rate controller for the F-16 VISTA. The performance of the controller is evaluated in Section 4 using parameter-space analysis as well as linear and nonlinear simulations. The final section provides a brief summary.

2. F-16 VISTA

VISTA is a modified F-16 with the capability of simulating advanced aircraft configurations and testing advanced flight control concepts. A detailed description of VISTA is given in [13]. In this section, an LPV model of the F-16 VISTA's short-period dynamics and the design objectives for an F-16 pitch-rate controller are reviewed. The same LPV model and design objectives were used to design LPV controllers in [18, 6] and a parameter-space controller in [5]. Utilizing the same model and specifications facilitates comparisons with previous work and better demonstrates the advantages of the procedure presented here.

2.1 LPV Model of the F-16 VISTA

The actual longitudinal dynamics of the VISTA aircraft vary significantly with flight condition (i.e. altitude h and Mach number M), and are denoted by $\mathcal{P}(h,M)$. For the pitch-rate control design, $\mathcal{P}(h,M)$ is modeled using the standard short period equations of motion (1) and a first order approximation of the actuator dynamics (2).

$$\frac{d}{dt}\begin{bmatrix}\alpha\\ q\end{bmatrix} = \begin{bmatrix}Z_\alpha & 1\\ M_\alpha & M_q\end{bmatrix}\begin{bmatrix}\alpha\\ q\end{bmatrix} + \begin{bmatrix}Z_{\delta_e}\\ M_{\delta_e}\end{bmatrix}\delta_{ed} \qquad (1)$$

where, α [deg] is the angle-of-attack, q [deg/s] is the pitch-rate, and δ_{ed} [deg] is the elevator deflection.

$$\begin{aligned}\delta_{ed} &= P_{act}\,\delta_{ec}\\ P_{act} &= \frac{-20.2}{s+20.2}\end{aligned} \qquad (2)$$

where, δ_{ec} is the elevator command. The negative sign in (2) is due to the sign convention used (i.e. a positive command produces a positive pitch-rate response).

At trimmed level flight, the dimensional coefficients Z_α, M_α, M_q, Z_{δ_e} and M_{δ_e} depend mainly on the altitude and Mach number. An LPV version of (1) for VISTA was developed by trimming and linearizing the Air Force Research Laboratory's high fidelity nonlinear simulation model of the F-16 VISTA at the operating conditions

$$M=[0.35\ 0.45\ 0.55\ 0.65\ 0.75\ 0.85]$$

$$h=[1{,}000\ 5{,}000\ 15{,}000\ 25{,}000]\ [\text{ft}]$$

and fitting the corresponding data for the dimensional coefficients with polynomial functions of h and M. The resulting expressions for the coefficients are given by (3) and shown in Figure 1.

$$\begin{aligned}
Z_\alpha(h,M) &= 0.22 - 4.1\cdot10^{-7}\cdot h - 2.6\cdot M + 5.15\cdot10^{-5}\cdot M\cdot h\\
M_\alpha(h,M) &= 17.1 - 8.07\cdot10^{-4}\cdot h - 68.4\cdot M\\
&\quad + 3.31\cdot10^{-3}\cdot M\cdot h + 56.2\cdot M^2 - 2.92\cdot10^{-3}\cdot M^2\cdot h\\
M_q(h,M) &= -0.228 + 7.06\cdot10^{-6}\cdot h - 2.12\cdot M\\
&\quad + 4.86\cdot10^{-5}\cdot M\cdot h\\
Z_{\delta_e}(h,M) &= -1.38\cdot10^{-3} + 8.75\cdot10^{-8}\cdot h - 0.34\cdot M\\
&\quad + 7.98\cdot10^{-6}\cdot M\cdot h\\
M_{\delta_e}(h,M) &= -8.16 + 1.73\cdot10^{-4}\cdot h + 40.6\cdot M\\
&\quad - 8.96\cdot10^{-4}\cdot M\cdot h - 99.3\cdot M^2 + 2.42\cdot10^{-3}\cdot M^2\cdot h
\end{aligned} \qquad (3)$$

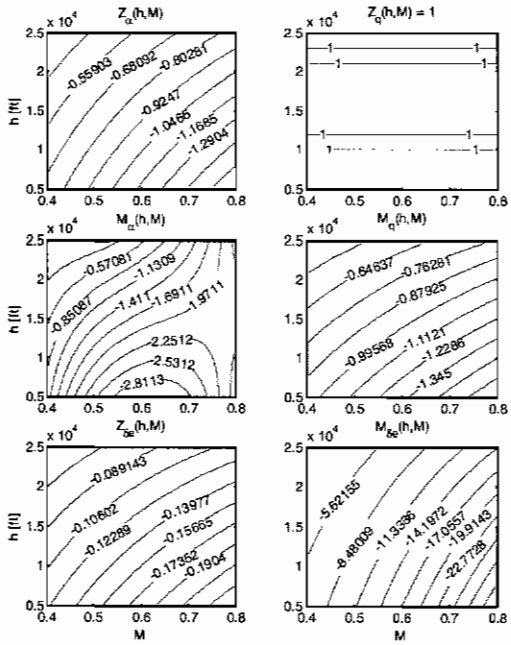

Figure 1: Dependence of the parameterized dimensional coefficients on flight condition.

Then, an LPV model of the short period equations of motion (4) is obtained when these polynomial expressions (3) are used with (1) and is given by

$$\frac{d}{dt}\begin{bmatrix}\alpha\\ q\end{bmatrix}=\begin{bmatrix}Z_\alpha(h,M) & 1\\ M_\alpha(h,M) & M_q(h,M)\end{bmatrix}\begin{bmatrix}\alpha\\ q\end{bmatrix}+\begin{bmatrix}Z_{\delta_e}(h,M)\\ M_{\delta_e}(h,M)\end{bmatrix}\delta_{ed} \quad (4)$$

and denoted by $P_{LPV}(h,M)$. Finally, the model used to represent $\mathcal{P}(h,M)$ for the pitch-rate control design is given by

$$P(h,M) = P_{LPV}(h,M)\cdot P_{act} \quad (5)$$

and accurately represents the F-16 VISTA's short period dynamics throughout the flight envelope $h \in$ [5,000; 25,000] [ft] and $M \in$ [0.4; 0.8]. Of course, even though $P(h,M)$ accurately represents $\mathcal{P}(h,M)$, there are obviously modeling errors, which results in model uncertainty denoted by Δ_m, where Δ_m represents the difference (in a multiplicative sense) between the actual aircraft dynamics and the model (5). That is, we assume

$$\mathcal{P}(h,M) = P(h,M)\cdot(1+\Delta_m) \quad (6)$$

The unstructured (i.e. non-parametric) uncertainty Δ_m is represented by

$$\Delta_m = W_u\cdot\Delta \quad (7)$$

where $\|\Delta\|_\infty \le 1$ and W_u defines the frequency dependent magnitude of the uncertainty Δ_m. Then, substituting (7) in (6) gives,

$$\mathcal{P}(h,M) = P(h,M)\cdot(1+W_u\cdot\Delta) \quad (8)$$

as depicted in Figure 2.

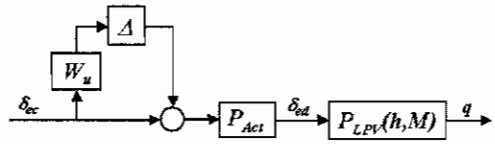

Figure 2: Block diagram representation of (8)

2.2 F-16 Pitch-Rate Control Design Objective

The objective is to design a controller for the F-16 VISTA that provides robust 'Level 1' pitch-rate command tracking throughout the design envelope $h \in$ [5,000; 25,000] [ft] and $M \in$ [0.4; 0.8] (i.e. the flight envelope for which (5) is valid). This design envelope includes a large part of the VISTA's test flight envelope[13], as shown in Figure 3. 'Level 1' (i.e. acceptable) time domain handling quality specifications for the pitch-rate response [12] are shown in Figure 4 and Table 1.

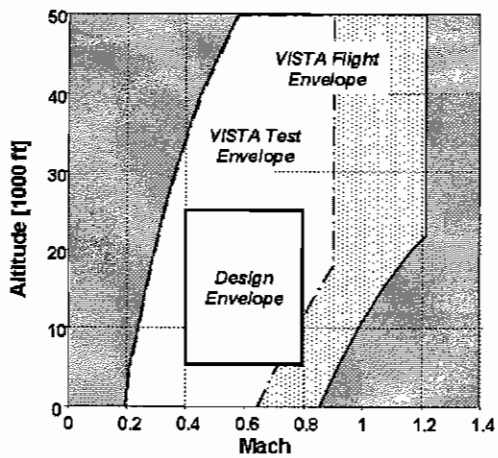

Figure 3: VISTA flight envelope

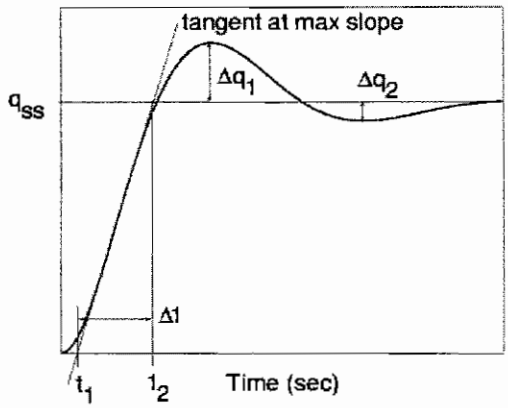

Figure 4: Pitch-rate Handling Quality Specifications

Table 1: Pitch-Rate Handling Quality Specifications		
Parameter	Level I	Level II
t_1 max	0.12 [s]	0.17 [s]
$\Delta q2/\Delta q1$ max	0.30	0.60
Δ_t max	$500/V_T$ [s]	$1600/V_T$ [s]
Δ_t min	$9/V_T$ [s]	$3.2/V_T$ [s]
V_T represents the true velocity [ft/sec]		

A reference model that satisfies the 'Level 1' pitch-rate 'Handling Quality Specifications' over the entire design envelope is given by,

$$P_d = \frac{4^2}{s^2 + 2 \cdot 0.5 \cdot 4 \cdot s + 4^2} \tag{9}$$

In the sequel, the reference model P_d will be referred to as the "desired dynamics". Then, the design objective can be satisfied by designing a controller that "forces" the closed-loop system to behave like the desired dynamics P_d throughout the design envelope.

3. Large Envelope Flight Control Design

In this section, a new approach for designing large envelope flight controllers for high performance aircraft is demonstrated by designing a pitch-rate controller for the F-16 VISTA. First, the control architecture is presented. Then, the design objective is formulated as an H_∞ control problem. Finally, MIMO H_∞ parameter-space design is used to design a robust pitch-rate controller that satisfies the design objective (i.e. provides a robust 'Level 1' pitch-rate response throughout the design envelope) with guaranteed H_∞ robust performance.

3.1 Control Architecture

The control architecture used here was first applied to large envelope flight control in [5] and is based on a "disturbance observer", which provides insensitivity to disturbances and model uncertainty. The disturbance observer architecture has been used successfully in a number of motion control applications[15,19,8,7,3]. Typically, a disturbance observer architecture incorporates a nominal plant model in the controller to estimate disturbances; however, as implemented here, this architecture is used to explicitly define the desired dynamics of the closed-loop, as shown in equation (16). The control architecture used here for the VISTA pitch-rate controller is shown in Figure 5,

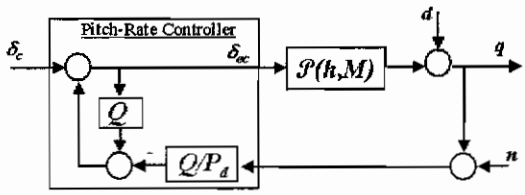

Figure 5: Pitch-rate controller architecture

where $\mathcal{P}(h,M)$ denotes the open-loop aircraft dynamics from elevator command to pitch-rate response and P_d denotes the desired pitch dynamics of the aircraft. The two filters P_d and Q form the pitch-rate controller when utilized as shown in Figure 5. In general, designing the 2DOF controller shown in Figure 5 would involve the design of both the filter Q and the desired dynamics P_d. However, as in this example, P_d is usually selected based on some knowledge of the desired closed-loop performance and independent of Q. Then, the objective is to design the filter Q so that a given pitch-rate command δ_c provides the desired response despite changing flight condition h-M, disturbances d, sensor noise n, and model uncertainty Δ_m. That is, design Q so that the closed-loop aircraft represented by Figure 5 has

$$q \simeq P_d \delta_c \tag{10}$$

as its input – output relation (within the frequency range of interest) throughout the design envelope.

Investigating the input-output transfer functions associated with the control architecture provides insight regarding the required form of Q and the expected characteristics of the resulting closed-loop. The loop-gain for the closed-loop aircraft represented by Figure 5 is

$$\hat{L}(h,M) = \frac{Q}{(1-Q)} \cdot \frac{\mathcal{P}(h,M)}{P_d} \tag{11}$$

The model regulation $\hat{H}$, disturbance rejection (sensitivity) $\hat{S}$, sensor noise rejection (complementary sensitivity) $\hat{T}$, and performance (error) $\hat{E}$ transfer functions of the controlled aircraft are given by

$$\hat{H}(h,M) \equiv \frac{q}{\delta_c} = \frac{P_d \cdot \mathcal{P}(h,M)}{P_d \cdot (1-Q) + \mathcal{P}(h,M) \cdot Q} \tag{12}$$

$$\hat{S}(h,M) \equiv \frac{q}{d} = \frac{1}{1+\hat{L}(h,M)} = \frac{P_d \cdot (1-Q)}{P_d \cdot (1-Q) + \mathcal{P}(h,M) \cdot Q} \tag{13}$$

$$\hat{T}(h,M) \equiv \frac{-q}{n} = \frac{\hat{L}(h,M)}{1+\hat{L}(h,M)} = \frac{\mathcal{P}(h,M) \cdot Q}{P_d \cdot (1-Q) + \mathcal{P}(h,M) \cdot Q} \tag{14}$$

$$\hat{E}(h,M) \equiv P_d - \hat{H}(h,M) \tag{15}$$

It is obvious from (12) – (14) that the design objectives can be satisfied by the selection of an appropriate low pass, unity gain filter for Q, which results in $q/\delta_c \rightarrow P_d$ and $q/d \rightarrow 0$ at low frequencies where $Q \rightarrow 1$ and $q/n \rightarrow 0$ at high frequencies where $Q \rightarrow 0$. In order to explicitly show the characteristics of this control architecture, Q is set to 1 in (12) and (13) and Q is set to 0 in (14) to obtain

$$\hat{H}_{Q=1}(h,M) = \frac{q}{\delta_c} = \frac{P_d \cdot \mathcal{P}(h,M)}{\mathcal{P}(h,M)} = P_d \tag{16}$$

$$\hat{S}_{Q=1}(h,M) = \frac{q}{d} = \frac{0}{\mathcal{P}(h,M)} = 0 \tag{17}$$

$$\hat{T}_{Q=0}(h,M) = \frac{-q}{n} = \frac{0}{P_d} = 0 \tag{18}$$

(16) and (17) clearly show that good model regulation and disturbance rejection are achieved within the bandwidth of Q, (despite variations in the aircraft dynamics $\mathcal{P}(h,M)$). Furthermore, (18) shows that the bandwidth of Q must be limited in order to reject high frequency sensor noise and to provide robustness to uncertainty (see (30)).

In order to design the filter Q using parameter-space design, it needs to be parameterized. The desired dynamics given by (9) mandate a Q filter with a relative degree of at least two for implementation purposes (causality of Q/P_d). Opting for a simple controller, the Q filter structure is chosen as

$$Q(\omega_Q, \zeta_Q) = \frac{\omega_Q^2}{s^2 + 2 \cdot \zeta_Q \cdot \omega_Q \cdot s + \omega_Q^2} \tag{19}$$

giving free design parameters ω_Q and ζ_Q.

3.2 H_∞ Control Problem Formulation

In this section, the VISTA pitch-rate control design problem (i.e. designing a controller that provides robust 'Level 1' pitch-rate responses throughout the design envelope) is formulated as an H_∞ design problem. In order to facilitate the "translation" of the handling quality and robustness specifications into H_∞ design specifications, the weighted design model shown in Figure 6 was developed. Similar weighted design models were used to design large envelope pitch-rate controllers for VISTA in [18, 6, 5].

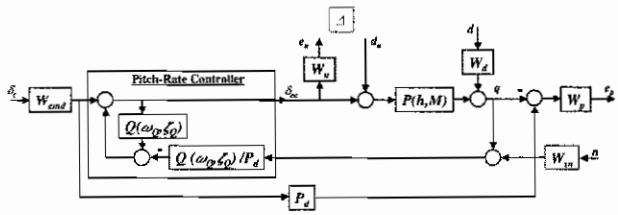

Figure 6: Weighted design model

The weighted design model incorporates the VISTA design model $P(h,M)$, its multiplicative uncertainty, and the 2DOF control architecture in a 'model matching' configuration. Using a 'model matching' configuration allows the handling quality specifications to be directly incorporated into the H_∞ design specifications by enabling the error between the closed-loop and the desired dynamics P_d to be directly penalized. The weights used in the design model are given by,

$$W_u = 2 \cdot \frac{s + 0.2 \cdot 1256}{s + 2 \cdot 1256} \quad \text{(Uncertainty Weight)} \tag{20}$$

$$W_p = 18 \cdot \frac{s}{(s+1)^2} \quad \text{(Performance Weight)} \tag{21}$$

$$W_{cmd} = \frac{10}{s+10} \quad \text{(Command Weight)} \tag{22}$$

$$W_d = \frac{0.7}{s+1} \quad \text{(Disturbance Weight)} \tag{23}$$

$$W_{sn} = 0.005 \quad \text{(Sensor Noise Weight)} \tag{24}$$

As discussed previously, the uncertainty weight W_u is used to account for the model uncertainties Δ_m in $P(h,M)$ (5), most notably unmodeled dynamics at high frequencies. W_u represents 20% modeling uncertainty at low frequencies and 200% at high frequencies. The performance weight W_p and the command weight W_{cmd} were motivated by the guidance given in [12], specifically regarding the typical frequency range of a pilot's commands and the frequency range of desired "model matching". Finally, the disturbance weight W_d and the

sensor noise weight W_{sn} were motivated by guidance given in [9].

Remark: Admittedly, the uncertainty weight (20) does not account for all of the dynamics neglected in the VISTA short period design model (5) (e.g. flexible modes). However, changing this weight to account for the neglected "mid-frequency" dynamics significantly changes the design problem, and makes comparisons with previous designs, which used similar uncertainty weights, impossible. Since the goal of the work presented in this paper was to demonstrate the proposed design method and its advantages over these previous design methods, similar design weights were used.

To facilitate notation in the sequel, the weighted design model in Figure 6 is represented by $N(h,M,\omega_Q,\zeta_Q)$ as shown in Figure 7.

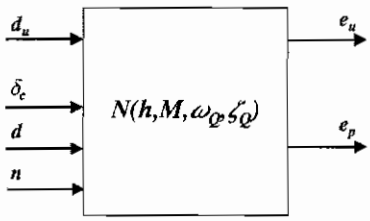

Figure 7: Compact representation of the weighted design model

Then, given the weighted design model $N(h,M,\omega_Q,\zeta_Q)$, the pitch-rate control design can expressed with the following two design specifications,

$$roots\{p_{cl}(h,M,\omega_Q,\zeta_Q)\} \subset \mathbb{C}^- \quad \text{(Nominal Stability)} \quad (25)$$

$$\left\| N(h,M,\omega_Q,\zeta_Q) \right\|_\infty \le 1 \quad \text{(Robust Performance)} \quad (26)$$

where, $p_{cl}(h,M,\omega_Q,\zeta_Q)$ in (25) represents the closed-loop characteristic equation.

Note that these design specifications depend on the flight condition h-M and the and the "free" parameters of the controller ω_Q-ζ_Q. Satisfying (25) and (26) at all flight conditions in the design envelope ensures that all of the roots of the nominal closed-loop are in the negative complex plane and that robust performance will be guaranteed throughout the design envelope; that is, it ensures that the closed-loop will remain stable and that the actual pitch-rate response will match the desired response to the accuracy specified by W_p despite changing flight condition h-M, disturbances d, sensor noise n, and the model uncertainty represented by W_u. While using the H_∞ norm to measure robust performance can be conservative, we have found that this conservatism is more than compensated for by the non-conservative explicit treatment of the flight condition parameters h and M.

In the next section, MIMO H_∞ parameter-space design will be used to find the feasible ω_Q-ζ_Q parameter set that satisfies (25) and (26) at all flight conditions in the design envelope. First, however, some additional insight regarding the required form of the Q filter can be obtained by looking at the two SISO transfer functions contained in the weighted design model corresponding to nominal performance (NP) and robust stability (RS), which are given by

$$\frac{e_p}{\delta_c} = W_p \cdot E(h,M,\omega_Q,\zeta_Q) \cdot W_{cmd} \quad \text{(NP)} \quad (27)$$

$$\frac{e_u}{d_u} = -W_u \cdot T(h,M,\omega_Q,\zeta_Q) \quad \text{(RS)} \quad (28)$$

Then, neglecting disturbances (d) and noise (n), the SISO H_∞ design specifications for nominal performance and robust stability are given by,

$$\left\| W_p \cdot E(h,M,\omega_Q,\zeta_Q) \cdot W_{cmd} \right\|_\infty \le 1 \quad \text{(Nominal Performance)} \quad (29)$$

$$\left\| W_u \cdot T(h,M,\omega_Q,\zeta_Q) \right\|_\infty \le 1 \quad \text{(Robust Stability)} \quad (30)$$

Note: E, and T in (27 – 30) are the same as $\hat{E}$, and $\hat{T}$ defined in Section 3.1, except that the actual VISTA longitudinal dynamics represented by $\mathcal{P}(h,M)$ is replaced by the design model of these dynamics $P(h,M)$ as defined in (5) and used in the weighted design model.

Examining (16) and (29) show that nominal performance is essentially quaranteed within the bandwidth of Q; however, examining (14), (18), and (30) shows that the bandwidth of Q must be limited in order to provide robust stability. Note that satisfying (26) ensures that both (29) and (30) are satisfied, and therefore, constraints imposed on the form of a feasible Q by (29) and (30) are also imposed by (26).

3.3 Parameter-Space Control Design

In this section, the MIMO H_∞ parameter-space design techniques of [1] are used to find the ω_Q-ζ_Q parameter set that satisfies the design specifications given by (25) and (26) at all flight conditions in the design envelope.

This is accomplished by mapping the "boundaries" of (25) and (26) into the ω_Q-ζ_Q parameter plane, where the "boundaries" define the condition that separates acceptable from unacceptable. For example, the

primary boundary for the nominal stability specification (25) is the imaginary axis, which separates stable closed-loop poles from unstable ones. The boundary for the robust performance specification (26) is the case when the H_∞ norm of the weighted design model equals one, which separates guaranteed robust performance from no guarantees. The details on mapping "boundaries" into parameter space for various control design specifications are given in [1]; however, in generic terms, mapping a boundary into parameter-space means solving for the parameters for which the "boundary conditions" are satisfied. Then, this set of parameters forms a "boundary" in parameter-space between the parameters that satisfy the specification and those that don't. Again, for example, mapping the nominal stability "boundary" involves solving for the parameters for which the characteristie equation has roots on the imaginary axis; sophisticated and efficient ways of doing that are given in [1]. Mapping the robust performance (i.e. MIMO H∞ norm) boundary directly would involve solving for the parameters for which the MIMO H∞ norm of the weighted design model is equal to one; however, interestingly enough, this boundary can be mapped using essentially the same techniques as used for the nominal stability case, since the MIMO H_∞ norm of the weighted design model is less than one if and only if its corresponding Hamiltonian matrix doesn't have any purely imaginary eigenvalues[1]. Thus, instead of solving for the parameter which cause the MIMO H_∞ norm to be one, this specification can be mapped by solving for the parameters for which a Hamiltonian matrix has eigenvalues on the imaginary axis, which is essential equivalent to the mapping involved to determine nominal stability[1].

After mapping both (25) and (26) into the ω_Q-ζ_Q parameter plane, the feasible region that simultaneously satisfies both requirements is formed by the intersection of the feasible region obtained from each individual requirement. Note that since (25) and (26) depend on flight condition *h-M*, the set of feasible ω_Q-ζ_Q satisfying these equations also depends on *h-M*. Since the objective is to design a controller that satisfies these specifications over the entire design envelope, (25) and (26) are mapped for as many operating conditions deemed necessary to ensure that the specifications are met throughout the design envelope; when the specifications are mapped at multiple flight conditions, the set of ω_Q-ζ_Q that satisfies the specifications at all flight conditions is formed by the intersection of the individual feasible regions obtained at each flight condition.

The region in the ω_Q-ζ_Q plane that satisfies (25) and (26) at the four "corners" of the design envelope is shown as the hatched regions in Figure 8. Note that for this design, the feasible region obtained by mapping the corners of the design envelope was not reduced by mapping additional flight conditions.

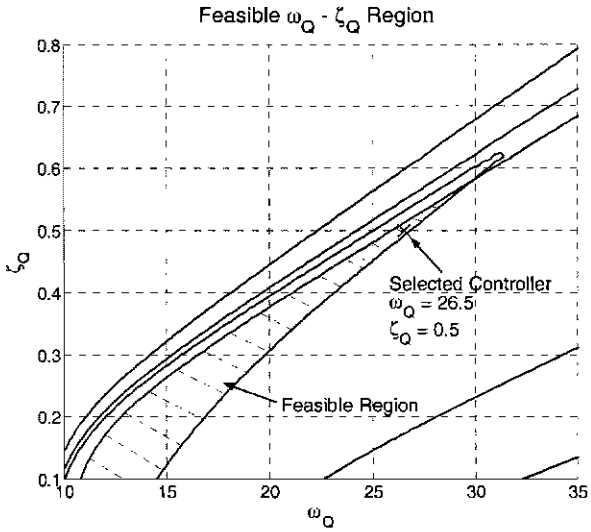

Figure 8: Feasible controller parameter region, which was formed by the intersection of the individual feasible regions obtained by mapping (25) and (26) into the ω_Q-ζ_Q plane at the four corners of the design envelope.

The design is completed by selecting one point from this feasible region. This can be done arbitrarily; however, if after mapping all design requirements, the feasible region is still large, additional demands can be placed on the controlled system. For example, the feasible solution that minimizes the structured singular value could be selected, or the original design specifications could be "tightened". Here, the final design, which is marked with an **x** in Figure 8, was chosen as ω_Q=26.5 rad/s and ζ_Q=0.7

4. Controller Evaluation

4.1 Verifying Flight Envelope

As indicated in the previous section, the feasible ω_Q-ζ_Q parameter region obtained by mapping (25) and (26) at the four corners of the design envelope was not reduced by mapping these specifications at additional flight conditions. However, since the LPV VISTA model used in the mapping equations is nonlinear, which is clear from (3) and Figure 1, there is a possibility of "missing" a region (possibly interior and small) of the design envelope for which the specifications are not satisfied. Therefor, after selecting a controller from the feasible controller parameter region, it is necessary to

verify that the selected controller does in fact satisfy (25) and (26) throughout the design envelope; this is easily done by mapping (25) and (26) into the flight envelope plane h-M with ω_Q and ζ_Q set to the selected controller; then, if the design envelope is contained in the feasible flight envelope, the specifications are guaranteed throughout the design envelope. The hatched region in Figure 9 shows the flight envelope for which the pitch-rate controller obtained with ω_Q=26.5 rad/s and ζ_Q=0.7 satisfies the design specifications. The design envelope, marked by the box in the Figure 9, is contained in the feasible h-M region, which confirms that the selected controller provides guaranteed robust performance (26) (which of course insures robust stability (30) as well) throughout the design envelope.

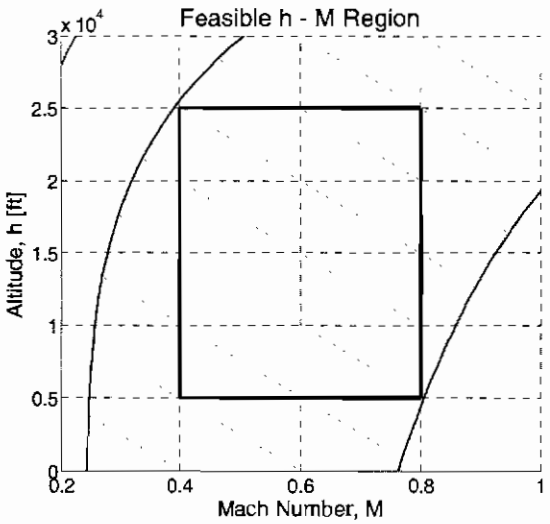

Figure 9: Flight envelope for which (25) and (26) are satisfied with ω_Q=26.5 rad/s and ζ_Q=0.7 is indicated by the hatched region.

4.2 Simulations Results

Linear simulation were preformed throughout the design envelope using the controller designed in the previous section. Figure 10 shows the VISTA's closed-loop response at the four corners of the design envelope; the figure also shows the pitch-rate command (the step) and the response of the desired dynamics P_d (9). These linear simulations clearly predict 'Level 1' handling qualities at the four extreme flight conditions. At three of the flight conditions, the pitch-rate response is essentially the same as the desired response. While the VISTA's response at h = 25,000 [ft] and M = 0.4 does have a little more overshoot than the desired dynamics, it is certainly within the 'Level 1' specifications.

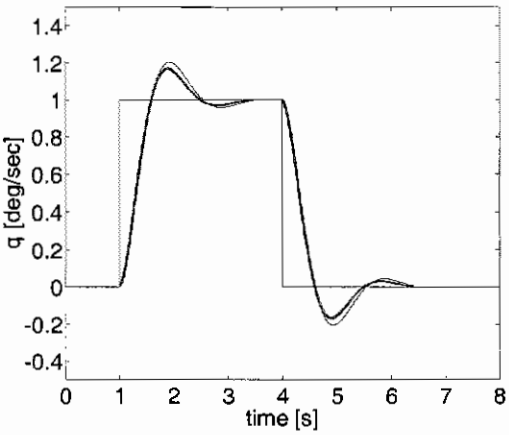

Figure 10. Linear simulation results

Nonlinear simulations were also performed, since achieving the desired performance in linear simulations is not sufficient when assessing the controlled dynamic behavior of the highly nonlinear F-16 VISTA aircraft. The nonlinear simulations also demonstrated a predicted 'Level 1' pitch-rate response throughout the design envelope. Figure 11 shows the simulation results when the maneuver starts at the center of the design envelope (i.e. h = 15,000 ft, M = 0.6).

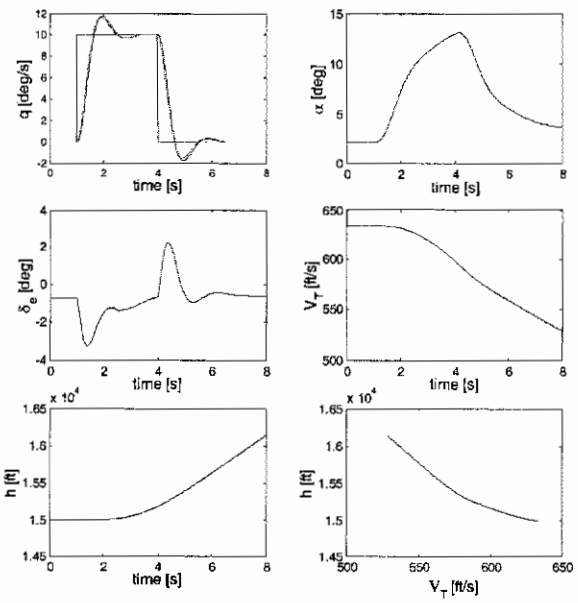

Figure 11: Nonlinear simulation results at the center of the design envelope.

5. Summary

A new method of designing large envelope controllers for high performance aircraft was presented. The procedure incorporates recent advances in MIMO H_∞ parameter-space control design to extend previous results so that robust performance can be guaranteed during the control design. The design method exploits the simplicity and transparency of a specific two-degree-of-freedom control architecture and the parameter-space design method to provide a straightforward means of designing robust large envelope flight controllers that provide explicitly defined desired closed-loop dynamics without gain-scheduling. The procedure was demonstrated by designing a large envelope pitch-rate controller for the F-16 VISTA aircraft. The resulting LTI controller was tested with both linear and nonlinear simulations and both predicted 'Level 1' handling qualities throughout the entire design envelope. This design example not only demonstrates the simplistic power of the proposed procedure, but also shows that it can yield an LTI controller when other methods cannot. The ability of the design procedure presented to provide such amazing results throughout large design envelopes without gain-scheduling is a result of both the control architecture used and the explicit, non-conservative treatment of varying/uncertain physical parameters in parameter-space H_∞ designs.

Acknowledgements

This research was supported in part by the Air Force Office of Scientific Research.

References

[1] J. Ackermann, P. Blue, T. Bünte, L. Güvenç, D. Kaesbauer, M. Kordt, M. Muhler, and D. Odenthal (2002). *Robust Control: the structural approach.* London: Springer.

[2] J. Ackermann, A. Barlett, D. Kaesbauer, W. Sienel, and R. Steinhauser (1993). *Robust control: Systems with uncertain physical parameters.* London: Springer.

[3] B. Aksun-Güvenç, T. Bünte, D. Odenthal, and L. Güvenç (2001). 'Robust two degree of freedom vehicle steering controller design', *Proc. of the American Control Conference*, Arlington.

[4] G. Becker (1993). *Quadratic Stability and Performance of Linear Parameter Dependent Systems.* Ph.D. thesis, Department of Mechanical Engineering, University of California, Berkeley.

[5] P. Blue, L. Güvenç, and Dirk Odenthal (2001). 'Large envelope flight control satisfying H_∞ robustness and performance specifications', *Proc. of the American Control Conference*, Arlignton.

[6] P. Blue and S. Banda (1997). 'D-K iteration with optimal scales for systems with time-varying and time invariant uncertainties'. *Proc. of the American Control Conference*, Albuquerque.

[7] T. Bünte, D. Odenthal, B. Aksun-Güvenç, and L. Güvenç (2001). 'Robust vehicle steering control based on the disturbance observer'. *Proc. of the 3rd IFAC Workshop on Advances in Automotive Control*, Karlsruhe.

[8] L. Güvenç and K. Srinivasan (1994). 'Friction compensation and evaluation for a force control application'. *J. of Mechanical Systems and Signal Processing*, vol. 8, uo. 6, pp. 623-638.

[9] Honeywell Technology Center (1996). "Application of multivariable control theory to aircraft control laws, Final Report: multivariable control design guidelines", *WL-TR-96-3099.*

[10] L. Lee (1997). Identification and Robust Control of Linear Parameter-Varying Systems. Ph.D. thesis, Department of Mechanical Engineering, University of California, Berkeley.

[11] W. Lu, K. Zhou, and J. Doyle (1991). 'Stabilization of LFT Systems', *Proc. of the Conference on Decision and Control*, Brighton, Eugland.

[12] MIL-STD-1797A (1990). *Military Standard – Flying Qualities of Piloted Vehicles.*

[13] J. Minor, A. Thurling, and E. Ohmit (2001). 'VISTA – a 21st century UAV testbed', *Proc. 32nd Society of Flight Test Engineers Symposium*, Seattle.

[14] D. Odenthal and P. Blue (2000). 'Mapping of frequency response magnitude performance specifications into parameter space'. *Proc. of the 3rd IFAC Symposium on Robust Control Design*, Prague.

[15] K. Ohnishi (1987). 'A new servo method in mechatronies'. *Trans. Japanese Soc. Elect. Eng.*, vol. 107-D, pp. 83-86.

[16] A. Packard (1994). 'Gain Scheduling via Linear Fractional Transformation', *Systems and Control Letters*, Vol. 22, pp. 79-92.

[17] J-Y. Shin and G. Balas (2002). 'Optimal blending functions in linear parameter varying control synthesis for F-16 aircraft'. *Proc. of the American Control Conference*, Anchorage.

[18] M. Spillman, P. Blue, L. Lee, and S. Banda (1996),=. 'A robust gain scheduling example using linear parameter varying feedback', *Proc. of the 13th IFAC World Congress*, San Francisco.

[19] T. Umeno and Y. Hori (1991), "Robust speed control of dc servomotors using modern two degrees-of-freedom controller design," *IEEE Trans. Ind. Electron.*, vol 38, no. 5, pp. 363-368.